

## Research Article

### Research on Thermal Error Compensation of Gear Hobbing Machine

<sup>1</sup>Qianjian Guo, <sup>1</sup>Shanshan Yu and <sup>2</sup>Jianguo Yang

<sup>1</sup>Shandong Provincial Key Laboratory of Precision Manufacturing and Non-Traditional Machining, Shandong University of Technology, Zibo 255049, China

<sup>2</sup>School of Mechanical Engineering, Shanghai Jiaotong University, Shanghai 200240, China

**Abstract:** The purpose of this research is to improve the machining accuracy of YK3610 Hobbing machine through thermal error compensation. This study presents the whole process of thermal error modeling and compensation by using Back Propagation Network (BPN) and ant colony optimization is introduced into the training of BPN. The results show that the BPN model based on ant colony algorithm improves the prediction accuracy of thermal errors on the gear hobbing machine and the thermal drift has been reduced from 14.2  $\mu\text{m}$  to 4.5  $\mu\text{m}$  after compensation.

**Keywords:** Ant colony algorithm, back propagation network, error compensation, thermal error modeling

#### INTRODUCTION

Among the sources of machine error, thermally induced errors account for 70 percent of the total errors, Ni (1997) presents real-time error compensation methods to reduce thermally induced machine tool errors. The mechanism causing the deformations of gear hobbing machine is so complex that the thermally induced errors are hard to predict. As a result, accurate modeling of thermal errors becomes the key step of error compensation. In recent years, a lot of research work concentrated on thermal error modeling has been conducted, such as successive regression analysis, different kinds of neural networks, grey system theory, multi-body system theory. Srinivasa and Ziegert (1996) develop a neural network model used to predict thermally induced errors in machine tools and the machine model is further tested using random thermal duty cycles. Ramesh *et al.* (2003) presents a hybrid Support Vector Machines-Bayesian Network model, the model is especially useful in a production environment wherein the machine tools are subject to a variety of operating conditions. Yang and Ni (2005) present a new modeling methodology for nonstationary machine tool thermal errors. The method uses the dynamic neural network model to track nonlinear time-varying machine tool errors under various thermal conditions. Chen (1996) presents a neural network model for on-line thermal error monitoring and the spindle thermal errors of a vertical machining centre were reduced by 70% after compensation. Gao *et al.* (2011) builds the relation between screw life and vibration features based on Compact Support Gaussian Fuzzy Neural Networks and

the parameters of the new model are optimized by an adaptive learning algorithm. Li *et al.* (2006) studies the optimization of thermal sensors' placement on machine tools based on grey correlation model of grey system theory. After optimization, the temperature variables in the thermal error' model are reduced from 16 to 4. Wang *et al.* (1998) presents a systematic methodology for the thermal-error correction of a machine tool and the thermal deformation is modeled using grey system theory so that a dynamic model can be obtained. In this study, BPN method based on Ant Colony Algorithm (BPN-ACO) is proposed to predict the thermal errors, which improves the accuracy of thermal error model. Finally, a high-accuracy thermal error compensation system based on the proposed BPN-ACO model has been developed to compensate for the thermal errors on YK3610 hobbing machine effectively.

#### EXPERIMENTAL SETUP

The experiment was implemented on YK3610 hobbing machine as shown in Fig. 1. To detect the temperature field of the machine tool, a total of 10 thermistors were installed and the locations of these thermistors can be divided into 7 groups:

- 1 Thermistor for measuring the bed temperature
- 2 Thermistor for measuring the guide way temperature
- 2 Thermistors for measuring the temperatures of hob spindle
- 2 Thermistors for measuring the temperatures of workpiece spindle

**Corresponding Author:** Qianjian Guo, Shandong Provincial Key Laboratory of Precision Manufacturing and Non-traditional Machining, Shandong University of Technology, Zibo 255049, China, Tel.: +86-533-2781723; Fax: +86-533-2781580

This work is licensed under a Creative Commons Attribution 4.0 International License (URL: <http://creativecommons.org/licenses/by/4.0/>).

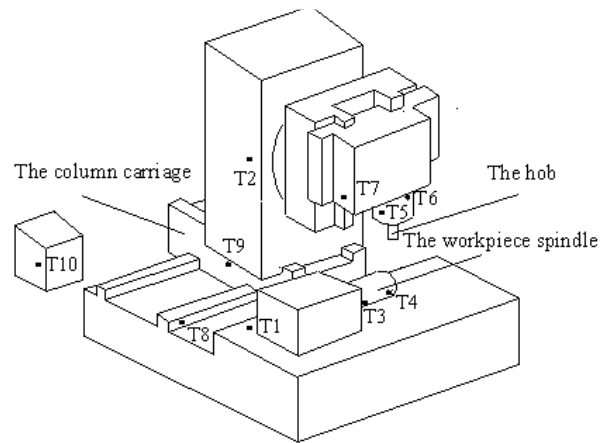


Fig. 1: The tested YK3610 hobbing machine

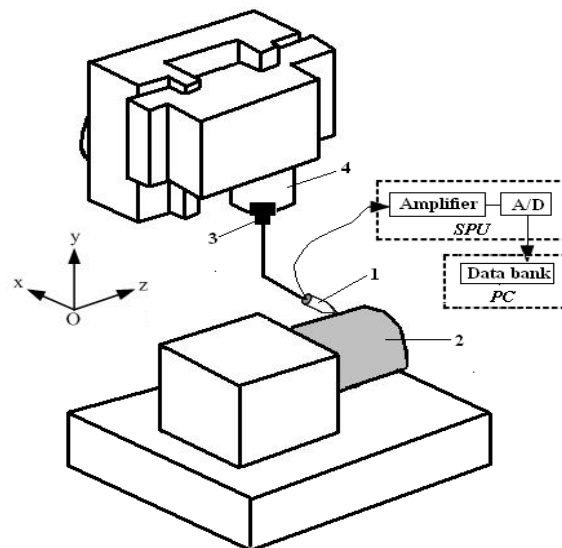


Fig. 2: The capacitance sensor mounted on the tool turret

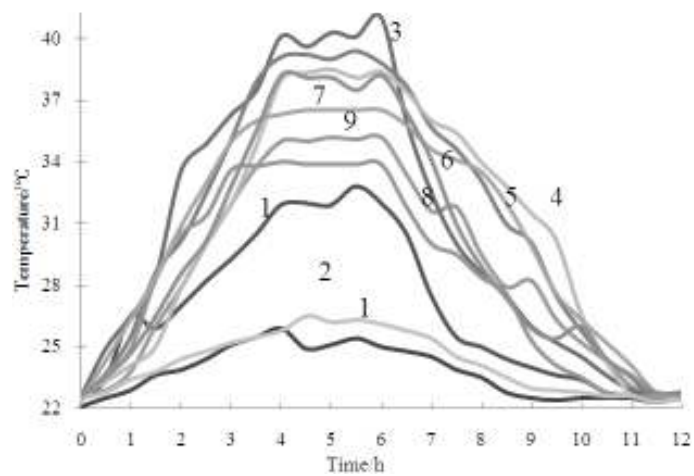


Fig. 3: Temperature histories of thermistor No. 1-10

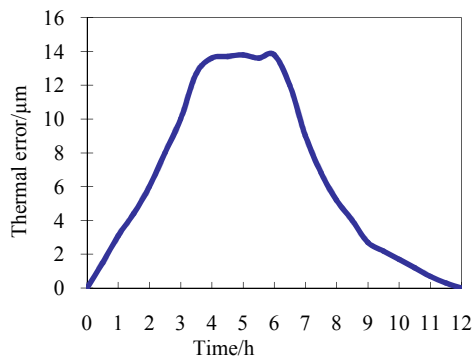


Fig. 4: Thermal errors of the spindle in the radial direction

- 1 Thermistors for measuring the temperatures of the column
- 1 Thermistor for measuring the temperature of the feed plate
- 1 Thermistor for measuring the temperature of the coolant tank

A capacitance sensor mounted on the tool turret was applied to measure the thermal drifts of the spindle in the x direction (the thermal errors of the spindle in the radial direction), as shown in Fig. 2.

First, an experiment was conducted to simulate the cycle of cutting a gear, in which the hob spindle was rotating at a speed of 1000 rpm, the workpiece spindle was rotating at a speed of 100 rpm and the coolant was flowing, but no gear was really processed. Initially, the gear hobbing machine ran for 4h. Then, the gear hobbing machine ran for another 2 h and then was cooled down for 6h. Under these working cycles, the temperature histories measured by thermistors (No.1-10) are shown in Fig. 3. Thermal error histories measured by the capacitance sensor are shown in Fig. 4.

### THERMAL ERROR MODELING

Artificial Neural Networks (ANN) are massively parallel information processing architectures composed of many simple, usually adaptive, processing elements interconnected to achieve specific collective computational capacities. The information is stored as weights and distributed throughout the interconnections of the network. The past few years have seen the development and practical application of ANNs in many fields. As a multilayered, fully connected, feed-forward network, BPN is used more widely than the other ANNs. The first layer of BPN network is called the input layer and the last layer is called output layer. Between the two layers is the hidden layer. By virtue of the computational structure, ANN possesses characteristics which are particularly attractive for the modeling of complicated and non-linear systems. The

performance of BPN is dependent on the several factors:

- The number of the hidden layers and the hidden nodes
- The learning rate and the momentum
- The number of the training data

Due to the characteristics of the gradient descent algorithm, BPN may converge to the local minimum of output error instead of the global minimum of output error, which induces the low convergence rate. To improve the performance, increase of hidden nodes (or layers), decrease of the momentum, the learning rate and the training data are suggested. Although sometimes the improvement is achieved at the price of computational cost, new solutions are still needed. In this study, ACO was introduced into the training of BPN.

In ant societies, the behaviors of the individuals are adaptive and robust, which are not regulated by any explicit form of centralized control. These complex behaviors are the result of self-organizing dynamics driven by local interactions and communications among a number of relatively simple individuals, which have made ant societies an attractive focus in recent years. Among the different works inspired by ant colonies, ACO is probably the most successful and popular one, which was firstly put forward by Marco Dorigo in 1990's and has been used successfully for solving complex optimization problems such as scheduling problems, traveling salesman problems. Zhao *et al.* (2011) presents the ant colony optimization algorithm.

ACO algorithm has the following components: a set of ant-like agents, the use of memory and stochastic decisions and strategies of collective and distributed learning. ACO draws its inspiration in the foraging behavior of ant colonies that, under appropriate conditions, are able to select the shortest path among few possible paths connecting their nest to a food source. The pheromone (a volatile chemical substance laid on the ground by the ants) is the mediator of this behavior, which affects in turn their moving decisions according to its local intensity while walking.

The basic idea of BPN-ACO can be explained as follows. After the structure of BPN is determined, the ants can be seen as input signals concurrently propagating through BPN and training the weights of the inter-neuron connections. The ants are locally propagated by means of a stochastic transfer function, the ant stochastic decision policy using only local information, the risk of being trapped in the local optima sharply decreases.

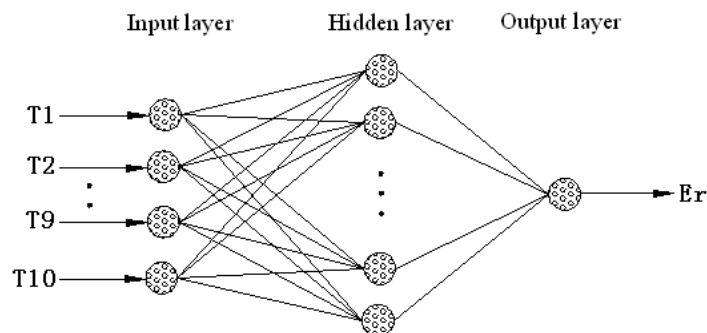


Fig. 5: The structure chart of BPN

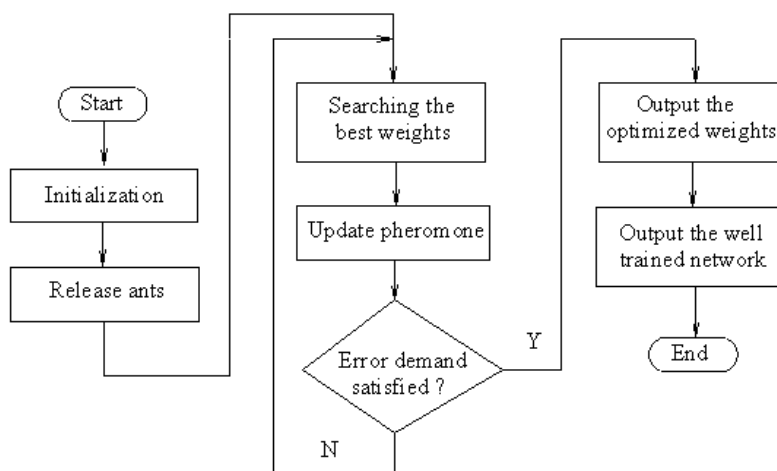


Fig. 6: The flowchart of BPN-ACO

Table 1: The parameters of BPN

The parameters of BPN	Value
Network structure	4-9-1
Initial weights	Random of (0, 1)
Learning rate	0.02
Momentum rate	0.5
Learning adjusting coefficients	0.8

Based on the analysis mentioned above, a three-layer BPN was adopted in this study to approximate thermal error in the radial direction. Ten neurons were used in the input layer to denote the ten temperature variables. One neuron was adopted in the output layer to represent thermal error. There are no perfect rules to determine the number of hidden nodes. The general procedure is by choosing a relative large number firstly and then the number is modified to satisfy the error demand. According to Kolmogorov theorem, the number of the hidden nodes is set as  $2N+1 = 2 \times 10 + 1 = 21$  finally (where  $N$  is the neuron number of the input layer). The BPN structure in this study was shown in Fig. 5. In the next section, 50 training samples were obtained from the thermistors and the capacitance sensor firstly. And then, the parameters of BPN were

set as listed in Table 1. Finally, ACO was used to adjust the 231 weights of BPN. The flowchart of BPN-ACO is shown in Fig. 6.

Suppose  $w_{ij}(1 = 1, 2 \dots 9, 10 j = 1, 2 \dots 21)$  is the weights between the input layer and the hidden layer,  $\phi_j (j = 1, 2 \dots 21)$  is the biases of hidden nodes,  $u_j (j = 1, 2 \dots 21)$  is the weights between the hidden layer and the output layer,  $\theta$  is the biases of the output node. Suppose  $s_{ij}(t)$  is the pheromone laid on path  $i \rightarrow j$  at moment  $t$ ,  $s_j(t)$  is the pheromone laid on path  $j \rightarrow OL$  (output layer) at moment  $t$ , which are used to simulate the pheromone intensity ants left. The training process includes the following steps:

- At the beginning of the training, 10 ants are allocated to the nodes of the input layer, the initial value of pheromone laid on path  $i \rightarrow j$  is defined as  $s_{ij}(0)$  and the initial value of pheromone laid on path  $j \rightarrow OL$  is defined as  $s_j(0)$ .
- Each  $w_{ij}$  composes a class called  $L_{w_{ij}}$ , each  $u_j$  composes a class called  $R_{u_j}$ . According to the pheromone intensity ratio, the ant chooses element

in  $L_{w_{ij}}$  and  $R_{u_j}$ . The probability of the ant chooses an element in  $L_{w_{ij}}$  and  $R_{u_j}$  is:

$$p_{w_{ij}}(t) = \frac{s_{L_{w_{ij}}}(t)}{\sum s_{L_{w_{ij}}}(t)} \quad (1)$$

$$p_{u_j}(t) = \frac{s_{R_{u_j}}(t)}{\sum s_{R_{u_j}}(t)} \quad (2)$$

where,

$S_{L_{w_{ij}}}(t)$  = The pheromone value of element in  $L_{w_{ij}}$  at moment t

$S_{R_{u_j}}(t)$  = The pheromone value of element in  $R_{u_j}$  at moment t

Finally, the element has maximum probability is chosen as the optimized weights.

- Next, the pheromone value of the optimized weights are adjusted according to the following equations:

$$s_{ij}(t + \Delta t) = \alpha * s_{ij}(t) + \sum_{n=1}^{10} \Delta s_{ij}^n \quad (3)$$

$$s_j(t + \Delta t) = \alpha * s_j(t) + \sum_{n=1}^{10} \Delta s_j^n \quad (4)$$

where,

$\alpha$  = The attenuation coefficient of the pheromone,

$\Delta t$  = The time step of choosing an element.

$\Delta s_{ij}^n$  = The pheromone left on path  $i \rightarrow j$  by ant n,  $\Delta s_j^n$  is the pheromone left on path  $j \rightarrow OL$  by ant n, the calculation rule is as follows:

$$\Delta s_{ij}^n = Q / e_{w_{ij}} \quad (5)$$

$$\Delta s_j^n = Q / e_{u_j} \quad (6)$$

where,

$Q$  = A constant used to adjust the growth rate of the pheromone

$e_{w_{ij}}$  = Maximum sampling error of the hidden nodes

$e_{u_j}$  = The maximum sampling error of the output node  $e = \max_{i=1}^m |y_i - o_i|$ ,  $m$ = The sample number

$Y_i$  = The expected output of the neural cells

$O_i$  = The practical output of the neural cells

According to the adjusting equation, the smaller the error, the faster the pheromone grows. When the

pheromone intensity reached a certain value, the error demand is met and the optimized weights are obtained. If the error demand can not be met, the training process returns to step 2).

### THERMAL ERROR COMPENSATION

The thermal error compensation system developed in this study was shown in Fig. 7. When the compensation was carried out, the temperature signals of the 10 key temperature points and the thermal error signals in the radial direction were measured with the thermistors and the capacitance sensor firstly. Then the signals were processed with the Signal Processing Unit (SPU, which is composed of DSP, amplifier, A/D board, serial port, parallel port, etc) and sent to the database of a PC through the serial port. In the next step, thermal error model was constructed using PC based on BPN method and the optimized model was sent back to DSP through the serial port. Finally, the compensation value was obtained by DSP and sent to CNC controller of the gear hobbing machine turning centre through the parallel port. After the feedback was added to the control signal of the servo loop, thermal error compensation came true at last.

In order to test the performance of the BPN-ACO model, one experiment was carried out. With the running of the developed system, 10 gears were machined on the YK3610 hobbing machine. The material of the workpieces was 45 steel. The hob spindle speed was set as 1000 rpm and the workpiece spindle speed was set as 100 rpm. During the experiment, the thermal errors were measured with the capacitance sensor and the predicted values were obtained using BPN-ACO model. Comparison of the measured value and the predicted values was shown in Fig. 8. It can be seen that the approximation ability of the model is very well, the residual error of the model is

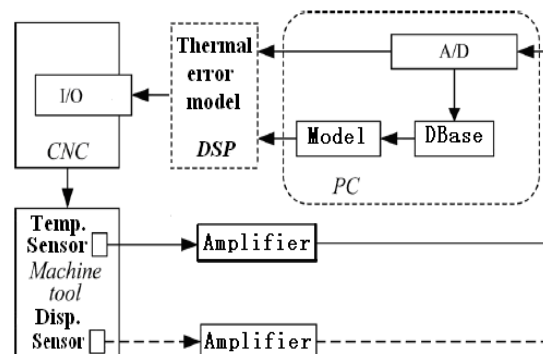


Fig. 7: Thermal error compensation system

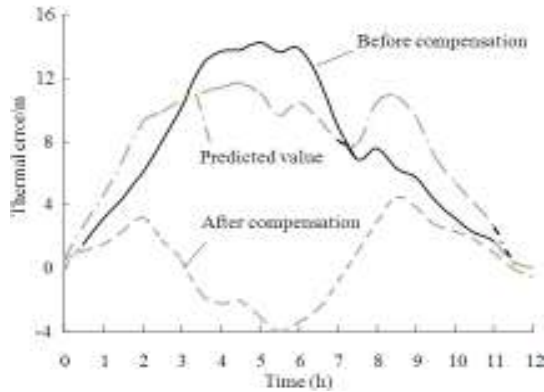


Fig. 8: The test results of the compensation system

smaller than 4.5  $\mu\text{m}$  and the compensation system is very effective.

### CONCLUSION

In this study, a BPN-ACO model was proposed for the prediction of the thermal errors on YK3610 hobbing machine. The approximation ability of the proposed BPN-ACO model is very well. During the performance test of the developed system, the thermal drift of the spindle in the x direction is reduced from 14.2  $\mu\text{m}$  to 4.5  $\mu\text{m}$  and the machining accuracy of the YK3610 hobbing machine is improved significantly.

### ACKNOWLEDGMENT

The authors gratefully acknowledge the financial support provided by the Project of Shandong Province Higher Educational Science and Technology Program (J11LD24) and the National Natural Science Foundation of China (51249001). Professor Jianguo Yang is gratefully acknowledged for his support during this study.

### REFERENCES

- Chen, J.S., 1996. Neural network-based modelling and error compensation of thermally-induced spindle errors. *Int. J. Adv. Manuf. Technol.*, 12: 303-308.
- Gao, H.L., X.C. Zhang and X.H. Shi, 2011. Screw life prediction based on accelerometer and compact support Gaussian fuzzy neural networks. *Sensor Lett.*, 9: 2043-2046.
- Li, Y.X., J.G. Yang and T. Gelvis, 2006. Optimization of measuring points for machine tool thermal error based on grey system theory. *Int. J. Adv. Manuf. Technol.*, 35: 745-750.
- Ni, J., 1997. CNC machine accuracy enhancement through real-time error compensation. *J. Manuf. Sci. Eng.*, 119: 717-725.
- Ramesh, R., M.A. Mannan and A.N. Poo, 2003. Thermal error measurement and modelling in machine tools. Part II. Hybrid bayesian network-support vector machine model. *Int. J. Mach. Tools. Manuf.*, 43: 405-419.
- Srinivasa, N. and J.C. Ziegert, 1996. Automated measurement and compensation of thermally induced error maps in machine tools. *Precis. Eng.*, 19: 112-132.
- Wang, Y., G. Zhang and K.S. Moon, 1998. Compensation for the thermal error of a multi-axis machining center. *J. Mater. Process. Technol.*, 75: 45-53.
- Yang, H. and J. Ni, 2005. Dynamic neural network modeling for nonlinear, nonstationary machine tool thermally induced error. *Int. J. Mach. Tools. Manuf.*, 45: 455-465.
- Zhao, X.H., D.L. Li and W.Z. Yang, 2011. Feature selection based on ant colony optimization for cotton foreign fiber. *Sensor Lett.*, 9: 1242-1248.